

## 钌(II)配合物 $[\text{Ru}(\text{dpq})_2\text{L}]^{4+}$ 的合成、晶体结构及与 G-四链体 DNA 的相互作用

孙 静<sup>\*1</sup> 宋兴栋<sup>1</sup> 陈文秀<sup>1</sup> 赵轩昊<sup>1</sup> 陈嘉曦<sup>1</sup> 贾振斌<sup>1</sup> 郝洪庆<sup>\*2</sup>

(<sup>1</sup> 广东医学院药学院, 东莞 523808)

(<sup>2</sup> 嘉应学院化学与环境学院, 梅州 514015)

**摘要:** 以  $\text{cis-}[\text{Ru}(\text{dpq})_2\text{Cl}_2] \cdot 2\text{H}_2\text{O}$  (dpq=二吡啶[3,2-d:2',3'-f]二氮杂)为原料与 5,5'-二(1-(三乙胺)甲基)-2,2'-联吡啶阳离子(L)合成钌(II)配合物 $[\text{Ru}(\text{dpq})_2\text{L}](\text{PF}_6)_4$ ,并研究了该配合物与 G-四链体 DNA 的作用;FRET 实验表明,配合物对人端粒 DNA h-telo 具有选择性,其作用能力要强于同癌基因启动子区域的四链 DNA,如 c-myc 和 bcl2;CD 光谱表明,在  $\text{Na}^+$ 和  $\text{K}^+$ 都不存在的情况下,配合物能诱导 h-telo 形成平行结构;此外,紫外和发射光谱都显示,配合物在  $\text{K}^+$ 溶液中与 h-telo 的作用力要大于在  $\text{Na}^+$ 溶液中的。

**关键词:** 钌(II)配合物; G-四链体; 选择性

中图分类号: O614.82<sup>†</sup>

文献标识码: A

文章编号: 1001-4861(2015)05-0865-08

DOI: 10.11862/CJIC.2015.142

## Synthesis, Crystal Structure and Interactions with G-Quadruplex Structures of $[\text{Ru}(\text{dpq})_2\text{L}]^{4+}$

SUN Jing<sup>\*1</sup> SONG Xing-Dong<sup>1</sup> CHEN Wen-Xiu<sup>1</sup> ZHAO Xuan-Hao<sup>1</sup>

CHEN Jia-Xi<sup>1</sup> JIA Zhen-Bin<sup>1</sup> HAO Hong-Qing<sup>\*2</sup>

(<sup>1</sup>School of Pharmacy, Guangdong Medical College, Dongguan, Guangdong 523808, China)

(<sup>2</sup>School of Chemistry and Environment, Jiaying University, Meizhou, Guangdong 514015, China)

**Abstract:** Based on  $\text{cis-}[\text{Ru}(\text{dpq})_2\text{Cl}_2] \cdot 2\text{H}_2\text{O}$  (dpq=dipyrido[3,2-d:2',3'-f]quinoxaline) and 5,5'-di(1-(triethylammonio)methyl)-2,2'-dipyridyl cation ligand (L), the complex  $[\text{Ru}(\text{dpq})_2\text{L}](\text{PF}_6)_4$  was synthesized and structurally characterized. The interactions of the complex with different G-quadruplexes were investigated. FRET melting assay proved that the complex bonds more strongly to h-telo than to promoters, such as c-myc and bcl2. CD studies show that Ru(II) complex can induce the formation of parallel G-quadruplex of h-telo in the absence of  $\text{Na}^+$  or  $\text{K}^+$ . Results of absorption and emission titration indicated that the complex has a higher DNA affinity with h-telo in  $\text{K}^+$  buffer than in  $\text{Na}^+$  buffer. CCDC: 945364.

**Key words:** Ru(II) complex; G-quadruplex DNA; selectivity

## 0 Introduction

Guanine-rich sequences of DNA have the propensity to form tetraplex structures known as G-quadruplexes, which are abundant in the human

telomere and in gene promoters<sup>[1-3]</sup>. There are more than 350000 guanine-rich sequences that can potentially form G-quadruplex DNA structures in the human genome<sup>[4-6]</sup>. Results have shown that formation of quadruplex in guanine-rich may play important

收稿日期: 2014-11-28。收修改稿日期: 2015-03-22。

国家自然科学基金(No.21101034),广东省优秀青年教师培养计划项目(No.Yq2013086,Yq2013151),东莞市科技计划项目(No.2011108102046),广东省大学生创新课题(No.1057112037)项目,2014 年广东省本科高校教学质量与教学改革工程立项建设项目资助。

\*通讯联系人。E-mail: sunjing03@foxmail.com; hqhao@126.com

roles in many biological functions, such as the inhibition of telomerase and the regulation of gene transcription and translation. The formation of G-quadruplex in the human telomere has been shown to inhibit telomerase which is an enzyme were expressed in over 80% cancer cells<sup>[7-9]</sup>. In the promoter regions the oncogenes, such as *c-myc* and *bcl2* are guanine rich, and formation of G-quadruplex in these regions has been proposed to regulate the corresponding oncogene's transcription<sup>[10-11]</sup>. Furthermore, G-quadruplex DNA has become a promising anticancer target. Over the past 10 years, there is considerable interest to develop small molecules that act as anticancer drugs by effectively stabilizing G-quadruplex<sup>[12-14]</sup>. It is an important goal to find new G-quadruplex binders that have selectivity between different G-quadruplex structures.

Metal complexes containing ruthenium(Ru) are an ideal platform for drug design and rationalization of structural interactions. Such complexes are appealing due to their electropositive, modular and facile synthesis, and interesting optical and magnetic properties. A number of Ru(II) complexes have been designed to target quadruplex DNA<sup>[13,15-16]</sup>. Previous studies have shown the great potential metal complexes have in binding to (and stabilizing) quadruplex, inhibiting telomerase, or regulating gene expression of certain oncogenes.

This work reports on the synthesis, characterization, selective interactions with G-quadruplex structures of a ruthenium(II) polypyridyl complex [Ru(dpq)<sub>2</sub>L]<sup>4+</sup> (dpq = dipyrro [3, 2-d:2', 3'-f]quinoxaline, L=5, 5'-di(1-(triethylammonio)methyl)-2,2' -dipyridyl cation). The obtained results will hopefully be of value in further G-quadruplex DNA recognition and binding by Ru(II) complexes and also lay foundation for rational design of new anticancer therapeutic agents.

## 1 Materials and methods

### 1.1 Materials

DNA oligomers 5'-AGGGTTAGGGTTAGGGTTA GGG-3'DNA (h-telo) was obtained from Sangon Biotechnology Company. The other reagents and solvents

were purchased commercially and used without further purification unless specially noted. Double distilled water was used to prepare buffer solutions. The formation procedure of intramolecular G-quadruplexes was carried out as follows: the oligonucleotide sample dissolved in a buffer solution that was heated to 95 °C for 5 min. The solution was then slowly cooled down to room temperature followed by incubation at 4 °C overnight. Buffer A contained 100 mmol·L<sup>-1</sup> KCl and 10 mmol·L<sup>-1</sup> Tris with pH 7.4; Buffer B contained 100 mmol·L<sup>-1</sup> NaCl and 10 mmol·L<sup>-1</sup> Tris with pH 7.4; Buffer C contained 10 mmol·L<sup>-1</sup> Tris with pH 7.4.

### 1.2 Physical measurement

Elemental analyses (C, H, and N) were carried out with a Perkin-Elmer 240C elemental analyzer. <sup>1</sup>H NMR spectra were recorded on a Varian Mercury-plus 300 NMR spectrometer with DMSO-d<sub>6</sub> as solvent and SiMe<sub>4</sub> as an internal standard at 300 MHz at room temperature. Electrospray ionization mass spectrometry (ESI-MS) was recorded on an LQC system (Finnigan MAT, USA) using CH<sub>3</sub>CN as mobile phase. UV-Visible (UV-Vis) and emission spectra were recorded on a Perkin-Elmer Lambda-850 spectrophotometer and Ls55 spectrofluorophotometer.

### 1.3 Preparation of ligands and complex

LBr<sub>2</sub>·4H<sub>2</sub>O<sup>[17]</sup>, 1,10-Phenanthroline-5,6-dione<sup>[18]</sup>, dpq<sup>[19]</sup> and *cis*-[Ru(dpq)<sub>2</sub>Cl<sub>2</sub>]·2H<sub>2</sub>O<sup>[20]</sup> were synthesized according to the literatures.

[Ru(dpq)<sub>2</sub>L](PF<sub>6</sub>)<sub>4</sub>·2H<sub>2</sub>O: A solution of *cis*-[Ru(dpq)<sub>2</sub>Cl<sub>2</sub>]·2H<sub>2</sub>O (0.27 g, 0.40 mmol) and LBr<sub>2</sub>·4H<sub>2</sub>O (0.25 g, 0.40 mmol) in ethylene glycol (30.0 cm<sup>3</sup>) was heated at 130 °C under the protection of argon for 6 h. In the process, the solution turned red. The solution was allowed to cool down to room temperature. After filtration, a drop-wise addition of saturated NH<sub>4</sub>PF<sub>6</sub> resulted in a deep red precipitate, which was further filtered. The crude product was recrystallized with CH<sub>3</sub>CN/CH<sub>3</sub>CH<sub>2</sub>OH (1:1, V/V), and red single crystals were obtained. Yield: 0.24 g (39%). Anal. Calcd. for C<sub>52</sub>H<sub>60</sub>O<sub>2</sub>F<sub>24</sub>N<sub>12</sub>P<sub>4</sub>Ru (1 566.04) (%): C, 39.88; H, 3.86; N, 10.73. Found(%): C, 40.07; H, 3.77; N, 10.80%. ESI-MS: *m/z* = 1 385.03 [M-PF<sub>6</sub>]<sup>+</sup> (44), 620.16 [M-2PF<sub>6</sub>]<sup>2+</sup> (100), 364.15 [M-3PF<sub>6</sub>]<sup>3+</sup> (86). <sup>1</sup>H NMR (DMSO-d<sub>6</sub>):

$\delta=9.62$  (d, 2H); 9.48 (d, 2H); 9.39 (dd, 4H); 9.07 (d, 2H); 8.50 (d, 2H); 8.27 (d, 2H); 8.16 (d, 2H); 8.09 (dd, 2H); 7.84 (dd, 2H); 7.72 (s, 2H); 4.29 (s, 4H); 2.99 (q, 12H); 0.97 (t, 18H).

#### 1.4 X-ray crystallography

Single crystal X-ray diffraction experiments were carried out with a Bruker Smart Apex CCD area detector at 153(2). The dimensions of complex crystals of the complex used for X-ray diffraction analysis were 0.34 mm  $\times$  0.21 mm  $\times$  0.08 mm. Data collection was performed with Cu  $K\alpha$  radiation ( $\lambda=0.154$  178 nm). Absorption corrections were applied by using the

SADABS program<sup>[21]</sup>. The structures were solved by direct methods, and all non-hydrogen atoms were refined anisotropically by least-squares on  $F^2$  using the SHELXTL program<sup>[22]</sup>. These were first refined isotropically and then anisotropically. The hydrogen atoms of the ligands were placed in calculated positions with fixed isotropic thermal parameters, and the structures factor calculations were included in the final stage of full-matrix least-squares refinement. A summary of the crystal data was given in Table 1.

CCDC: 945364.

Table 1 Crystallographic data of [Ru(dpq)<sub>2</sub>L](PF<sub>6</sub>)<sub>4</sub>·2H<sub>2</sub>O

Empirical formula	C <sub>52</sub> H <sub>60</sub> O <sub>2</sub> F <sub>24</sub> N <sub>12</sub> P <sub>4</sub> Ru	$Z$	2
Formula weight	1 566.03	$D_c / (\text{g} \cdot \text{cm}^{-3})$	1.559
Crystal system	Triclinic	$F(000)$	1 576
Space group	$P\bar{1}$	$\theta$ range for data collection / (°)	2.803~66.989
$a / \text{nm}$	1.319 75(7)	Limiting indices	$-8 \leq h \leq 15, -19 \leq k \leq 19, -18 \leq l \leq 20$
$b / \text{nm}$	1.635 29(9)	Reflections collected	22 781
$c / \text{nm}$	1.710 32(8)	Independent reflections	11 526 ( $R_{\text{int}}=0.035$ 0)
$\alpha / (^\circ)$	74.732(4)	Goodness-of-fit on $F^2$	1.05
$\beta / (^\circ)$	69.203(4)	$R_1, wR_2$ ( $I > 2\sigma(I)$ )	0.066 7, 0.202 1
$\gamma / (^\circ)$	82.865(4)	$R_1, wR_2$ (all data)	0.073 9, 0.212 9
Volume / nm <sup>3</sup>	3.326 9(3)	$(\Delta\rho)_{\text{max}}, (\Delta\rho)_{\text{min}} / (\text{e} \cdot \text{nm}^{-3})$	2 451, -743

#### 1.5 FRET melting assay

The fluorescent labeled oligonucleotide h-telo (5'-FAM-AG<sub>3</sub>[T<sub>2</sub>AG<sub>3</sub>]<sub>3</sub>-TAMRA-3', FAM: 6-carboxyfluorescein, TAMRA: 6-carboxy-tetramethylrhodamine), c-myc (5'-FAM-[TG4AGGGTGGGGAGGGTGGGGAAGG]-TAMRA-3') and bcl2 (5'-FAM-AGGGGCGGGCGCGGAGAGGAAGGGGCGGGAGCGGGGCTG-3'-TAMRA) were used as the FRET (Fluorescence Resonance Energy Transfer) probes. They were diluted in 60 mmol·L<sup>-1</sup> potassium cacodylate buffer (pH 7.4) and then annealed by heating to 95 °C for 5 min, followed by slow cooling to room temperature overnight. Fluorescence melting curves were determined with a Roche Light Cycler II real-time PCR machine. The total reaction volume is 20  $\mu\text{L}$ , with a series of different concentrations of the complex and 0.2  $\mu\text{mol} \cdot \text{L}^{-1}$  of labeled oligonucleotide. Measurements were made on a RT-PCR with excitation at 470 nm and detection at 530 nm. Fluorescence readings were taken at intervals

of 1 °C over the range of 37~99 °C, with a constant temperature being maintained for 30 s prior to each reading to ensure a stable value.

#### 1.6 CD studies

A circular dichroism (CD) study was conducted to observe the effect of the complex on the structure of the h-telo G-quadruplex. CD studies were performed on a JASCO J-810 spectropolarimeter at room temperature. Spectral data were collected at 0.2 nm intervals with a scan speed of 200 nm·min<sup>-1</sup> three times at each CD spectrum. The oligomers were resuspended in Tris-HCl buffers A, B, and C. CD spectra were baseline-corrected for signal contributions due to the buffer. Then CD titration was performed at a fixed DNA concentration (3  $\mu\text{mol} \cdot \text{L}^{-1}$ ) with various concentrations of the complex. All solutions were mixed thoroughly and allowed to equilibrate for 5 min before data collection (until no elliptic changes were observed).

### 1.7 Absorption and emission spectra

The absorption and emission titration of the Ru(II) complex in buffers A and B were performed using a fixed complex concentration, to which increments of the DNA stock solution were added. The concentration of  $[\text{Ru}(\text{dpq})_2(\text{L})]^{4+}$  solution was  $10 \mu\text{mol} \cdot \text{L}^{-1}$ , and the volume was 3 mL. Complex-DNA solutions were allowed to incubate for 5 min before the spectra were recorded. The titration processes were repeated several times until no change was observed in the spectra, indicating that binding saturation was achieved. Changes in the Ru(II) complex concentration due to dilution at the end of each titration were negligible.

### 1.8 Continuous variation analysis

Binding stoichiometries were obtained for the complex using the method of continuous variation<sup>[23-24]</sup>. The concentrations of the Ru(II) complex and DNA varied, while the sum of the concentrations of the two reactants was kept constant at  $10 \mu\text{mol} \cdot \text{L}^{-1}$ . In the solutions, the mole fraction of Ru(II) complex varied from 0 to 1 in 0.1 increments. Each mixture was equilibrated at 4 °C for 12 h in the dark. The fluorescence intensities of these mixtures were measured at 25 °C using an excitation wavelength of 443 nm. The  $F_{\text{max}}$  (fluorescence) was recorded in the range of 500~750 nm. Binding stoichiometries were obtained from the intercepts of linear plot obtained by linear least-squares fits to the left- and right-hand portions of the Job's plot.

## 2 Results and discussion

Fig.1 depicts the structure of the complex. Selected bond distances and bond angles are given in Table 2. The complex contains a six-coordinated

ruthenium atom chelated by two dpq ligands and one dicationic L ligand. The coordination geometry about the ruthenium atom is a distorted octahedron, with a bite angle of  $79.5^\circ$  averaged over three bidentate ligands. This distortion from an ideal octahedral geometry is due to the customary narrow bite angles of the bipyridine moieties, as observed in some other ruthenium complexes<sup>[25-26]</sup>. The mean Ru-N bond length for the complex (0.206 2 nm) is typical value for this type of Ru(II) complexes (0.205 9~0.206 9 nm)<sup>[27-28]</sup>. The torsion angle between tpyridine pairs of two bpy ligands of the complex is nonequivalent ( $3.1^\circ$ ).

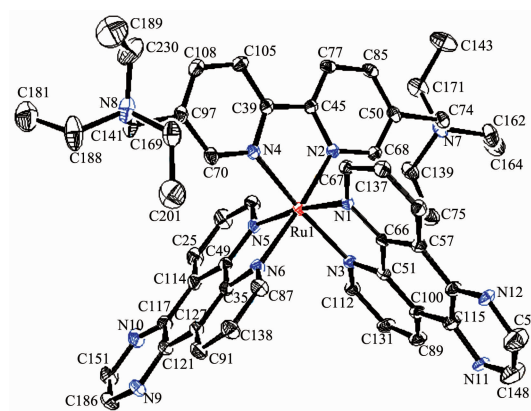
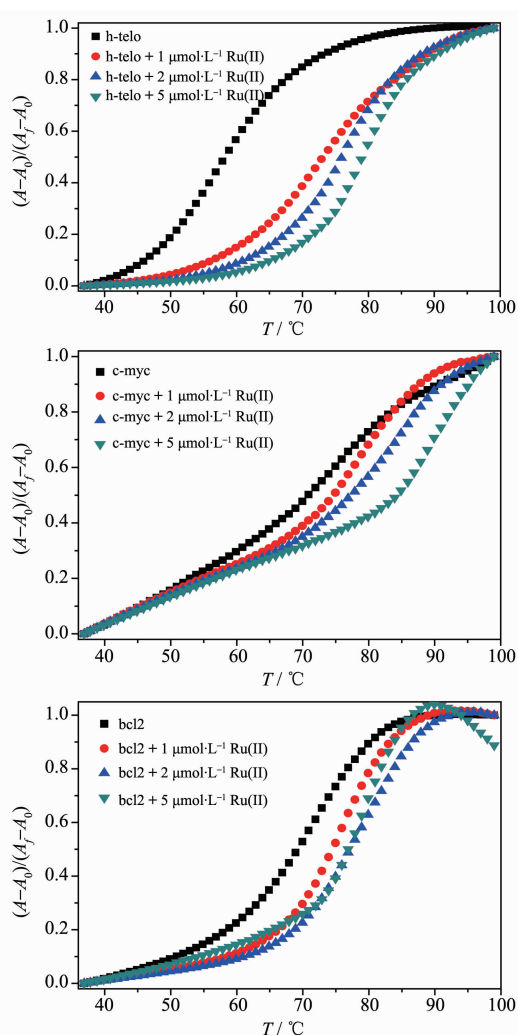


Fig.1 X-ray crystal structure of  $[\text{Ru}(\text{dpq})_2\text{L}]^{4+}$  showing non-hydrogen atoms with 30% probability thermal ellipsoids

FRET studies were conducted to investigate the binding abilities of the compound to h-telo, promoter G-quadruplex DNA sequences, c-myc and bcl2. Reliable FRET melting curves (Fig.2) and stabilization temperature ( $\Delta T_m$ ) values (Table 3) were obtained<sup>[29]</sup>. As shown in Table 3, the complex exhibits selectivity to h-telo G-quadruplex DNA at all three different concentrations. For example, it had  $\Delta T_m$  values  $>20^\circ\text{C}$

Table 2 Selected bond lengths (nm) and angles ( $^\circ$ ) for metal environments of  $[\text{Ru}(\text{dpq})_2\text{L}](\text{PF}_6)_4 \cdot 2\text{H}_2\text{O}$

Ru(1)-N(1)	0.207 0(4)	Ru(1)-N(2)	0.204 9(4)	Ru(1)-N(3)	0.206 4(4)
Ru(1)-N(4)	0.204 7(4)	Ru(1)-N(5)	0.206 7(4)	Ru(1)-N(6)	0.207 3(4)
N(1)-Ru(1)-N(2)	90.11(15)	N(1)-Ru(1)-N(3)	80.05(15)	N(1)-Ru(1)-N(4)	95.47(15)
N(1)-Ru(1)-N(5)	172.03(16)	N(1)-Ru(1)-N(6)	94.38(15)	N(2)-Ru(1)-N(3)	98.06(16)
N(2)-Ru(1)-N(4)	79.00(16)	N(2)-Ru(1)-N(5)	96.22(16)	N(2)-Ru(1)-N(6)	174.53(15)
N(3)-Ru(1)-N(4)	174.69(14)	N(3)-Ru(1)-N(5)	94.23(15)	N(3)-Ru(1)-N(6)	85.80(16)
N(4)-Ru(1)-N(5)	90.50(15)	N(4)-Ru(1)-N(6)	97.45(16)	N(5)-Ru(1)-N(6)	79.58(16)



$C_{\text{DNA}}=0.2 \mu\text{mol}\cdot\text{L}^{-1}$ ,  $C_{\text{Ru}}=1, 2$  and  $5 \mu\text{mol}\cdot\text{L}^{-1}$ ;  $\lambda_{\text{em}}=530 \text{ nm}$ ,  $\lambda_{\text{ex}}=470 \text{ nm}$

Fig.2 FRET-melting curves for experiments carried out with h-telo, c-myc and bcl2 separately with [Ru(dpq)<sub>2</sub>L]<sup>4+</sup>

**Table 3 Stabilization temperatures,  $\Delta T_m$  for h-telo, c-myc and bcl2 stabilized by [Ru(dpq)<sub>2</sub>L]<sup>4+</sup> determined from FRET**

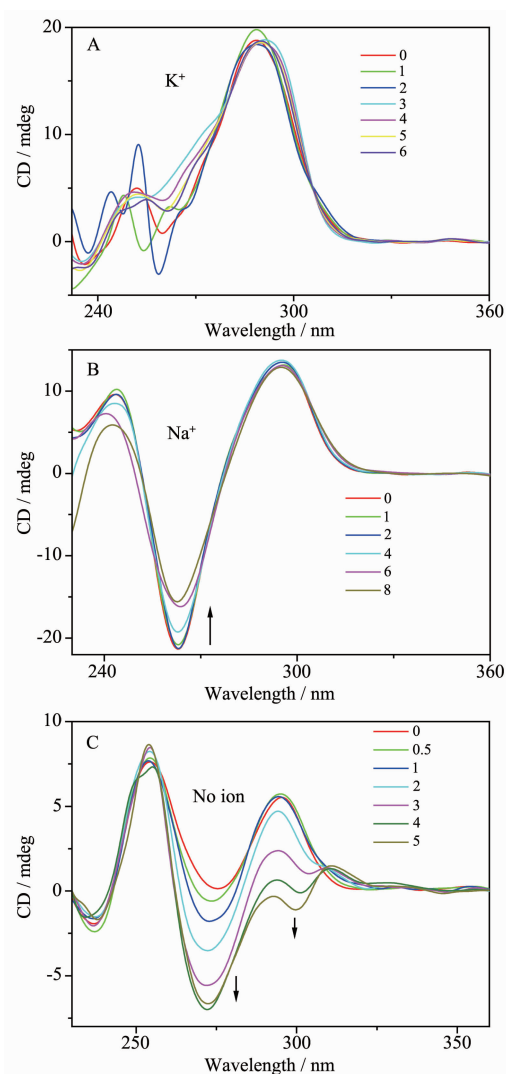
$C_{\text{complex}} / (\mu\text{mol}\cdot\text{L}^{-1})$	$\Delta T_m / ^\circ\text{C}$		
	h-telo	c-myc	bcl2
1	15.0	4.0	4.2
2	18.8	10.0	5.8
5	21.8	14.4	7.4

with h-telo G-quadruplex; in contrast, the complex had  $\Delta T_m$  values  $<15^\circ\text{C}$  with c-myc and  $\Delta T_m$  values  $<8^\circ\text{C}$  with bcl2 at  $5 \mu\text{mol}\cdot\text{L}^{-1}$ . Therefore, the complex might be considered as a good selective G-quadruplex binder to distinguish different G-quadruplexes.

CD spectroscopy was employed to determine the solution formation of h-telo G-quadruplex and confirm a transformation of G-quadruplex induced by Ru(II) complex. H-telo G-quadruplexes generally form a mixed conformation (parallel/antiparallel) in  $\text{K}^+$  solution<sup>[30-32]</sup>. The CD spectrum exhibited a large positive band at 290 nm, a small positive band at 250 nm, and a negative band at 235 nm. On the other hand, the CD spectrum of the same sequence in the presence of  $\text{Na}^+$  ions had a 295 nm positive band and a 265 nm negative band, which was characteristic of an antiparallel G-quartet structure<sup>[33-34]</sup>. In the absence of metal cations, the CD spectrum of the h-telo sequence indicated the coexistence of a single strand and two types of quadruplex structures, parallel and antiparallel G-quadruplexes<sup>[30-35]</sup>. As shown in Fig.3, no obvious spectral changes were observed upon addition of the complex to h-telo in buffer  $\text{K}^+$  or  $\text{Na}^+$  solution. This implies that the conformation of G-quadruplex was stabilized by  $\text{K}^+$  or  $\text{Na}^+$ , and the complex could not change the conformation of G-quadruplex at high ionic strength. Without any metal cations, the CD spectra of h-telo exhibited a negative band centered at 235 nm, a major positive band at 255 nm, and a rather broad positive signal around 295 nm. Addition of the complex decreased the CD intensity of the band at 295 nm (antiparallel G-quadruplex) and increased the band at 255 nm (parallel G-quadruplex), demonstrating that the Ru(II) complex can induce and stabilize the formation of parallel G-quadruplex in the absence of metal cations. At the same time, a strong positive band at 310 nm started to appear. The induced CD signal suggested that, in addition to the end-stacking mode, other binding modes (i.e., phosphate back-bone binding or H-bond interactions) are also possible<sup>[36]</sup>.

Absorption spectra titration was performed to determine the binding affinity of the complex to h-telo. The UV-Vis spectrum of the complex consists of three well resolved bands between 250~550 nm. The ultraviolet band around 255 nm and 293 nm can be attributed to intraligand (IL) transition, and the visible band appearing at 443 nm was assigned to metal-to-ligand charge transfer (MLCT) according to the spectra



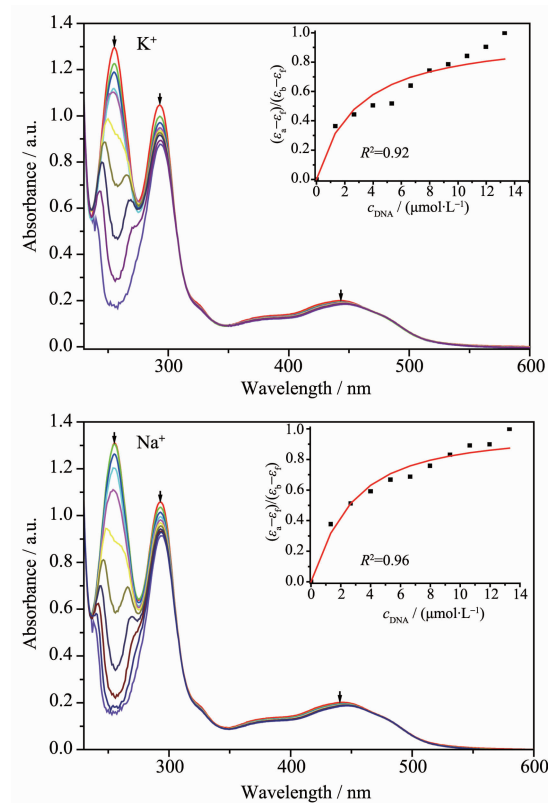


$r = C_{\text{Ru}} / C_{\text{DNA}}$ ; A:  $r = 0 \sim 6$  ( $\text{K}^+$ ); B:  $r = 0 \sim 8$  ( $\text{Na}^+$ ); C:  $r = 0 \sim 5$  (No ion)

Fig.3 CD spectra of G-quadruplex induced by  $[\text{Ru}(\text{dpq})_2\text{L}]^{4+}$  with a  $3 \mu\text{mol} \cdot \text{L}^{-1}$  h-telo in buffer A, B and C at room temperature

of other  $\text{Ru}(\text{II})$  complexes<sup>[37]</sup>. The electronic spectral trace of the complex with successive increase of h-telo at room temperature in  $\text{K}^+$  or  $\text{Na}^+$  buffer is given in Fig.4. The absorption intensities of all the three bands mentioned above successively decrease and show red

shift upon addition of DNA. The MLCT absorption shifts from 442 to 447 nm ( $\Delta\lambda = 5$  nm) with 7.87% hypochromism in  $\text{K}^+$  buffer, and the MLCT absorption shifts from 443 to 447 nm ( $\Delta\lambda = 4$  nm) with 7.33% hypochromism in  $\text{Na}^+$  buffer. The others and related quantitative data are shown in Table 4.



$C_{\text{Ru}} = 10 \mu\text{mol} \cdot \text{L}^{-1}$ ,  $C_{\text{DNA}} = 0 \sim 14 \mu\text{mol} \cdot \text{L}^{-1}$  from top to bottom; Inset: plot of  $(\varepsilon_a - \varepsilon_i) / (\varepsilon_b - \varepsilon_i)$  vs  $C_{\text{DNA}}$  and the nonlinear fit for the titration of DNA to  $\text{Ru}(\text{II})$  complex

Fig.4 Absorption spectra of  $[\text{Ru}(\text{dpq})_2\text{L}]^{4+}$  in  $\text{K}^+$  and  $\text{Na}^+$  buffer in the presence of h-telo

In order to compare the DNA-binding affinities of the complex quantitatively, the intrinsic binding constants  $K_b$  of DNA are obtained from monitoring changes in the MLCT absorbance for the complex. In

Table 4 Absorption spectra and DNA-binding constants  $K_b$  of  $[\text{Ru}(\text{dpq})_2\text{L}]^{4+}$

Buffer	$\lambda_{\text{max}}(\text{free}) / \text{nm}$	$\lambda_{\text{max}}(\text{bound}) / \text{nm}$	$\Delta\lambda / \text{nm}$	$H / \%$	$K_b / (\text{L} \cdot \text{mol}^{-1})$	$s$
$\text{K}^+$	442	447	5	7.87	$(2.08 \pm 0.21) \times 10^4$	$0.08 \pm 0.06$
	293	293	0	16.28		
	255	258	3	87.14		
$\text{Na}^+$	443	447	4	7.33	$(0.98 \pm 0.10) \times 10^4$	$0.18 \pm 0.10$
	293	295	2	13.70		
	254	257	3	88.39		

equation **1**,  $C_{\text{DNA}}$  is the DNA concentration in nucleotides;  $\varepsilon_a$  is the extinction coefficient observed for the MLCT absorption band at a given DNA concentration;  $\varepsilon_f$  and  $\varepsilon_b$  are the extinction coefficients for the free Ru(II) complex and Ru(II) complex in the fully bound form, respectively<sup>[37-40]</sup>;  $K_b$  is the equilibrium binding constant;  $C_t$  is the total Ru(II) complex concentration;  $s$  is the binding site size. Equations **1a** and **1b** are applied to absorption titration data for non-cooperative metalointercalators binding to DNA.

$$(\varepsilon_a - \varepsilon_f) / (\varepsilon_b - \varepsilon_f) = [b - (b^2 - 2K_b^2 C_t C_{\text{DNA}} / s)^{1/2}] / (2K_b C_t) \quad (1a)$$

$$b = 1 + K_b C_t + K_b C_{\text{DNA}} / (2s) \quad (1b)$$

From the decay of the absorbance, the intrinsic binding constants  $K_b$  of the complex in  $\text{K}^+$  and  $\text{Na}^+$  buffer were  $(2.08 \pm 0.21) \times 10^4 \text{ L} \cdot \text{mol}^{-1}$  and  $(0.98 \pm 0.10) \times 10^4 \text{ L} \cdot \text{mol}^{-1}$ , respectively. Greater  $K_b$  is observed for the complex upon addition of the mixed-hybrid quadruplex DNA ( $\text{K}^+$ ) than for the antiparallel basket quadruplex DNA ( $\text{Na}^+$ ) under the same conditions; this indicates stronger interaction between the DNA bases and the complex.

The results of the luminescence titration of  $[\text{Ru}(\text{dpq})_2(\text{L})]^{4+}$  with h-telo are illustrated in Fig.5. The complex can display luminescence in  $\text{K}^+$  and  $\text{Na}^+$  buffer at ambient temperature with a maximum appearing at 627 nm. The fluorescence intensity of  $[\text{Ru}(\text{dpq})_2(\text{L})]^{4+}$  increased with the increase of DNA concentration. The maximum ratio reached at  $C_{\text{DNA}} / C_{\text{Ru}} \approx 1.4$  at which there is a 1.87- and 1.46-fold increase in the fluorescence intensity in  $\text{K}^+$  and  $\text{Na}^+$  buffer, respectively. The results also indicate that the complex binds the mixed-hybrid quadruplex more avidly than that of antiparallel basket quadruplex DNA, which is consistent with the results obtained by absorption spectra titrations.

The method of continuous variation known as Job's plot was used in order to determine the stoichiometry interactions between the complex and G-quadruplex DNA. Fig.6 shows the Job's plot of the complex with h-telo in  $\text{K}^+$  or  $\text{Na}^+$  buffer. Two major inflection points for the complex were observed at  $x = 0.45$  in  $\text{K}^+$  buffer and at  $x = 0.53$  in  $\text{Na}^+$  buffer. It is evident that the binding ratio is determined to be 1:1.

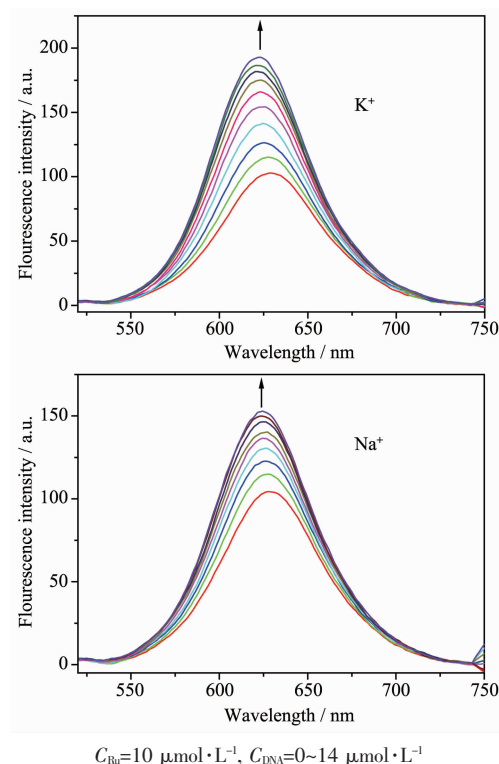


Fig.5 Luminescence spectra of  $[\text{Ru}(\text{dpq})_2\text{L}]^{4+}$  in  $\text{K}^+$  and  $\text{Na}^+$  buffer in the presence of increasing amounts of h-telo

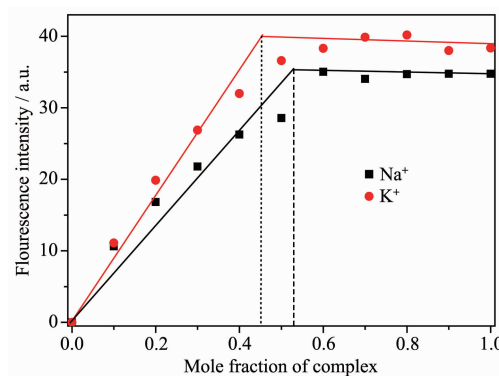


Fig.6 Job's plot using luminescence data for  $[\text{Ru}(\text{dpq})_2\text{L}]^{4+}$  and h-telo in  $\text{K}^+$  (●) and  $\text{Na}^+$  (■) buffer

This binding stoichiometry suggests that each complex molecule interacts with each molecule of G-quadruplex DNA<sup>[41]</sup>.

### 3 Conclusions

One Ru(II) complex  $[\text{Ru}(\text{dpq})_2(\text{L})]^{4+}$  has been synthesized and characterized. It has a good selectivity for h-telo G-quadruplex and has a higher DNA affinity in  $\text{K}^+$  buffer than in  $\text{Na}^+$  buffer. The 1:1 stoichiometry suggests that each complex molecule

interacts with each molecule of G-quadruplex DNA.

## References:

- [1] Huppert J L, Balasubramanian S. *Nucleic Acids Res.*, **2005**, **33**:2908-2916
- [2] Huppert J L. *Chem. Soc. Rev.*, **2008**, **37**:1375-1384
- [3] Murat P, Singh Y, Defrancq E. *Chem. Soc. Rev.*, **2011**, **40**: 5293-5307
- [4] Huppert J L, Balasubramanian S. *Nucleic Acids Res.*, **2007**, **35**:406-413
- [5] Todd A K, Johnston M, Neidle S. *Nucleic Acids Res.*, **2005**, **33**:2901-2907
- [6] Reed J E, White A J P, Neidle S, et al. *Dalton Trans.*, **2009**: 2558-2568
- [7] Kim N W, Piatyszek M A, Prowse K R, et al. *Science*, **1994**, **266**:2011-2015
- [8] Shay J W, Bacchetti S. *Eur. J. Cancer*, **1997**, **33**:787-791
- [9] Kelland L R. *Anticancer Drugs*, **2000**, **11**:503-513
- [10] Suntharalingam K, Gupta D, Miguel P J S, et al. *Chem. Eur. J.*, **2010**, **16**:3613-3616
- [11] Finkel T, Serrano M, Blasco M A. *Nature*, **2007**, **448**:767-774
- [12] Bertrand H, Monchaud D, Cian A D, et al. *Org. Biomol. Chem.*, **2007**, **5**:2555-2559
- [13] SUN Jing(孙静), CHEN Jia-Xi(陈嘉曦), LIN Hai-Ling(林海玲), et al. *Chinese J. Inorg. Chem.* (无机化学学报), **2012**, **28**:45-49
- [14] Jain A K, Paul A, Maji B, et al. *J. Med. Chem.*, **2012**, **55**: 2981-2993
- [15] Chen X, Wu J H, Lai Y W, et al. *Dalton Trans.*, **2013**:4386-4397
- [16] Shi S, Huang H L, Gao X, et al. *J. Inorg. Biochem.*, **2013**, **121**:19-27
- [17] An Y, Lin Y Y, Wang H, et al. *Dalton Trans.*, **2006**:2066-2071
- [18] Paw W, Eisenberg R. *Inorg. Chem.*, **1997**, **36**:2287-2293
- [19] Collins J G, Sleeman A D, Aldrich-Wright J R, et al. *Inorg. Chem.*, **1998**, **37**:3133-3141
- [20] Deshpande M S, Kumbhar A A, Kumbhar A S, et al. *Bioco-njugate Chem.*, **2009**, **20**:447-459
- [21] Sheldrick G M. *SADABS*, University of Göttingen, Germany, **1996**.
- [22] Sheldrick G M. *SHELXS-97 and SHELXL-97*, University of Göttingen, Germany, **1996**.
- [23] Haq I, Lincoln P, Suh D, et al. *J. Am. Chem. Soc.*, **1995**, **117**:4788-4796
- [24] Haq I, Trent J O, Chowdhry B Z, et al. *J. Am. Chem. Soc.*, **1999**, **121**:1768-1779
- [25] Santra B K, Menon M, Pal C K, et al. *Dalton Trans.*, **1997**: 1387-1393
- [26] Sun J, Wu S, An Y, et al. *Polyhedron*, **2008**, **27**:2845-2850
- [27] Rillema D P, Jones D S, Woods C, et al. *Inorg. Chem.*, **1992**, **31**:2935-2938
- [28] Khatua S, Samanta D, Bats J W, et al. *Inorg. Chem.*, **2012**, **51**:7075-7086
- [29] Mergny J L, Maurizot J C. *ChemBioChem*, **2001**, **2**:124-132
- [30] Rezler E M, Seenisamy J, Bashyam S, et al. *J. Am. Chem. Soc.*, **2005**, **127**:9439-9447
- [31] Ambrus A, Chen D, Dai J X, et al. *Nucleic Acids Res.*, **2006**, **34**:2723-2735
- [32] Xu Y, Noguchi Y, Sugiyama H. *Bioorg. Med. Chem.*, **2006**, **14**:5584-5591
- [33] Antonacci C, Chaires J B, Sheardy R D. *Biochemistry*, **2007**, **46**:4654-4660
- [34] Dai J X, Punchihewa C, Ambrus A, et al. *Nucleic Acids Res.*, **2007**, **35**:2440-2450
- [35] Li W, Wu P, Ohmichi T, et al. *FEBS Lett.*, **2002**, **526**:77-81
- [36] Zheng X H, Zhong Y F, Tan C P, et al. *Dalton Trans.*, **2012**: 11807-11812
- [37] Chen L M, Liu J, Chen J C, et al. *J. Inorg. Biochem.*, **2008**, **102**:330-341
- [38] Carter M T, Rodriguez M, Bard A J. *J. Am. Chem. Soc.*, **1989**, **111**:8901-8911
- [39] Maheswari P U, Palaniandavar M. *J. Inorg. Biochem.*, **2004**, **98**:219-230
- [40] Shi S, Geng X T, Zhao J, et al. *Biochimie*, **2010**, **92**:370-377
- [41] Rajput C, Rutkaite R, Swanson L, et al. *Chem. Eur. J.*, **2006**, **12**:4611-4619